JOURNAL OF MATERIALS SCIENCE 29 (1994) 47–53

Some aspects of crack initiation in mild steel under corrosion fatigue condition

G. P. RAY
76 Stillness Road, London SE23 1NF, UK
R. A. JARMAN
School of Engineering, University of Greenwich, London SE18 6PF, UK
J. G. N. THOMAS
The Round House, Parkmill, Swansea SA3 2EE, UK

The initiation of corrosion fatigue cracks has been studied for mild steel tested in 0.6 M sodium chloride solution. The results indicate that cyclic stress enhances the formation and coalescence of micropits at, and around, the inclusions, leading to the nucleation of cracks. Dissolution of the inclusions promotes local transport of hydrogen into the metal. Hydrogen plays a significant role in the initiation of voids and microcracks. Crack initiation also occurs with the formation of voids in and around slip bands, at grain boundaries and in the pearlitic regions.

1. Introduction

The influence of aqueous environment and cyclic stress or strain on the initiation of environmentally sensitive fracture is still a matter of considerable debate. In many engineering alloys cracks may nucleate at some weakly constrained interface or at stress concentrations associated with discontinuities, such as non-metallic inclusions, in the structure. Significant changes in solution composition, however, can occur at or near such discontinuities. Hence, the effects of non-metallic inclusions in the initiation of corrosion fatigue cracks are as likely to be related to their influence on local electrochemical effects as to any related to stress intensification [1].

Sulphide inclusions present in the material act as sites for H_2S generation [2–4] and low-energy paths for hydrogen diffusion into the material. The presence of hydrogen assists nucleation of microcracks at inclusion sites, grain boundaries and carbides in the pearlite [4]. In addition, localized corrosion rapidly occurs in the vicinity of the non-metallic inclusions developing voids or micropits. The crevices and subsequent pits tend to serve as sites for crack initiation.

The work reported here concerns an investigation concerning some aspects of crack initiation in smooth-surfaced En1-type mild steel specimens carried out in 0.6M sodium chloride solution at room temperature. Results of an earlier study using scanning electron microscopy (SEM) are described elsewhere [5, 6]. In this paper, results of an examination using transmission electron microscopy (TEM) are presented. Some of the earlier results [6] are also further analysed in the light of additional evidence.

2. Experimental procedure

The material used for this investigation was commercially available En1-type mild steel details of which are given in Table I. The test specimens were made from wrought mild steel bars, sectioned parallel to the rolling direction, and were of 9.6 cm gauge length and 7.5 mm gauge diameter. Some specimens were annealed at 920 °C for 3 h in argon. All specimens were ground with successive grades of silicon carbide papers followed by polishing to a 1 μm finish. Some specimens were also electropolished in 10% perchloric acid mixture.

Inclusions present at the surface of the mild steel were analysed using an electron probe microanalyser (EPMA), model Jeol 3A. Samples of the polished steel were immersed in 0.6M sodium chloride solution for up to 20 h followed by examination of the surfaces using SEM and X-ray spectra (EDAX). Corrosion fatigue tests were performed in Schenck rotating bending machines at 47 Hz for varying lengths of time. The stresses applied to the specimens ranged from 95–309 MPa.

A sodium chloride solution prepared from laboratory grade chemical dissolved in deionized water to 0.6M concentration and of pH 6.5, was drip-fed on to the centre of the rotating specimens through a PTFE nozzle. The distance between the specimen surface and the nozzle was kept to a minimum. The solution temperature was maintained at 22 °C.

In order to study the change in surface morphology of the specimens due to straining, fatigue tests were interrupted at various intervals to obtain plastic replicas for observation using TEM.

Immediately after the interruption of each test, the specimen was cleaned in 1% triammonium citrate solution, *in situ*, to remove corrosion products and chloride ions from the surfaces and crevices [7], washed in deionized water followed by alcohol. Indirect carbon replicas were obtained using a standard

0022–2461 © *1994 Chapman & Hall*

TABLE I Nominal Composition and Mechanical Properties of Steel

Elements	Composition (%)
C	0.11
Mn	0.41
Si	0.016
S	0.037
P	0.018
Cr	0.05
Ni	0.02
UTS: 565–596 MPa	
Elongation: 9%–13%	
Reduction of area: 48%–57%	

technique. In each case two plastic replicas were made. The first was discarded, its function being to clean the surface, and the second was used in the production of a carbon replica. Gold–palladium alloy was deposited at an angle of 45° after the initial deposition of carbon. The shadowed carbon replicas were examined using TEM, replicas being taken from the longitudinal surface of the specimen.

Some of the fatigue-tested specimens were also examined using optical microscopy, SEM and EDAX.

3. Results

Results of immersion tests in 0.6M sodium chloride solution for up to 20 h showed corrosion at the inclusion–matrix interface. The EDAX analysis results indicated the presence of sulphur and manganese in the inclusion, and sulphur, manganese and iron at the inclusion–matrix interface.

On the application of cyclic stress, 95 MPa, R (stress ratio) $= -1$, formation and coalescence of micropits at the inclusion–matrix interface and generation of etch pits on the matrix were found to occur. Some of the inclusions also appeared to dissolve. In addition, slip-band formation and nucleation of microfissures in the transverse direction at the inclusion–matrix interfaces were observed. As the number of the reversals was increased, the formation of microfissures at the slip bands, fracture of some of the inclusions and increasing dissolution in the sulphur-enriched bands surrounding the inclusions, appeared to occur.

Further increase in the number of reversals showed formation of slip bands between the pearlitic regions, micropits within the slip bands and microcracks around pearlitic colonies. Localized attack at the ferrite–cementite interfaces resulting in the formation of microvoids and terminations and bends in the cementite lamellae in the pearlitic regions were found to occur (Fig. 1a). Extrusion–intrusion effects associated with grain boundaries, formation of hydrogen blisters in the vicinity of many inclusions irrespective of the shape, size or chemical composition of the inclusions, and nucleation of intrusions in the region of high blister density were observed in the as-received as well as in the annealed specimens (Fig. 1b). The formation of subgrains and microcracks at subgrain boundaries, deformed regions with microcracks and etch pits associated with distorted regions are illustrated in Figs 1c, 2a and b, respectively. Grain-boundary deformation causing nucleation of microcracks was also found to occur with increasing number of reversals.

At 179 MPa, $R = -1$, dissolution along grain boundaries and pearlitic regions was observed (Fig. 3).

At 193 MPa, $R = -1$, microcracks associated with hydrogen blisters near inclusions (Fig. 4a), voids caused by intersecting slip bands and hydrogen blisters (Fig. 4b), and dissolution at the ferrite–cementite interface resulting in the formation of microvoids in the ferrite, were observed after 2000 reversals. With an increasing number of reversals, dissolution of the inclusions and microvoid formation in the slip bands also appeared to occur. In the low-density regions, deformation and microcrack formation at the grain boundaries, and slip bands with micropits were observed. As the number of reversals was further increased, linking up of microcracks at the grain boundaries and around the inclusions were found to occur.

In the electropolished specimens, similar surface morphologies, i.e. intrusion–extrusion effects at the grain boundaries and microcrack formation at slip bands present between pearlitic regions, were observed.

When the cyclic stress was increased to 247 MPa, $R = -1$, corrosion in the pearlitic areas and around elongated and spherical inclusions were also seen. Initiation of microfissures in the transverse direction at the inclusion–matrix interface were found to occur due to the intersection of the slip bands and the inclusions (Fig. 5). Increasing the number of reversals enhanced the tendency for coalescence of incipient cracks along the grain boundaries, of micropits in the slip bands and the nucleation of microcracks in the transverse direction from the inclusion–matrix interface.

With further increase in cyclic stress, it was observed that corrosion occurred rapidly at the inclusion–matrix interface. Corrosion also occurred in the sulphur-enriched bands surrounding the inclusions causing microvoids (Fig. 6). Coalescence of these microvoids resulted in the nucleation of incipient cracks in the transverse direction at the inclusion–matrix interfaces. Increasing the stress to 309 MPa, $R = -1$, appeared to enhance the mechanical effect rather than the corrosive one, in that the fracture and spalling of the inclusions tended to occur more readily. Voids on the matrix in the vicinity of slip bands caused by mechanical effect are shown in Fig. 7.

4. Discussion

In this investigation, it was observed that the surface of the specimen contained regions of high and low densities of inclusions which were sulphides of manganese only, or of manganese and iron. Examination of surfaces using TEM did not indicate the presence of voids or crevices at the inclusion–matrix interfaces before the commencement of the tests. However, it was observed that the inclusions were surrounded by a

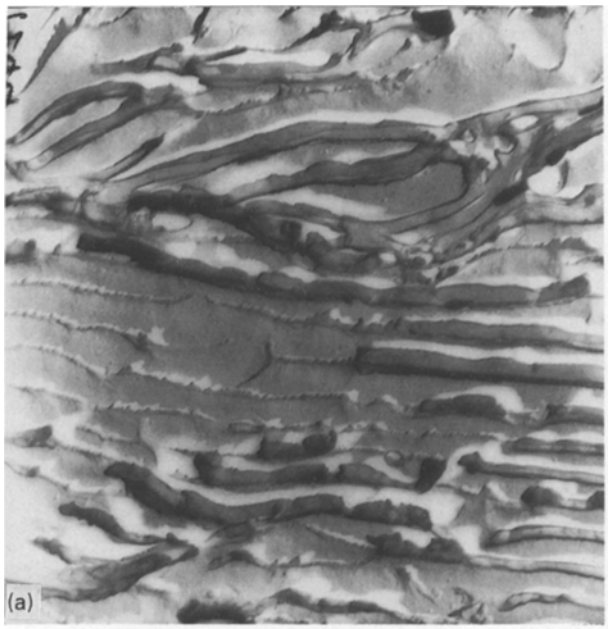

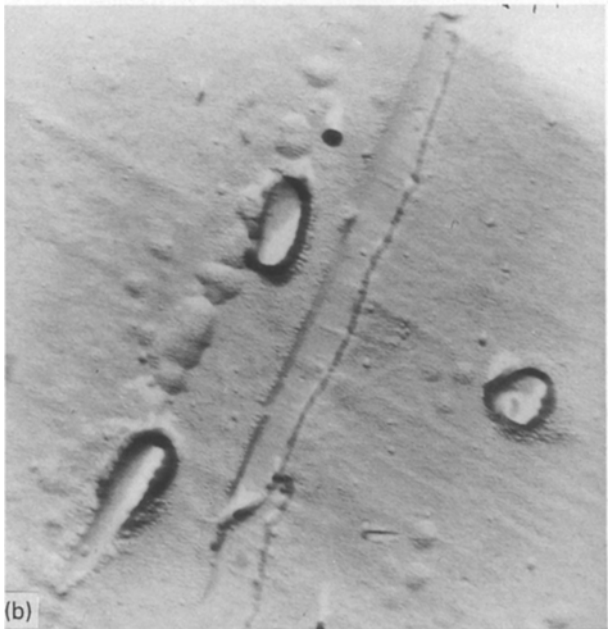

Figure 1 Transmission electron micrograph of an annealed specimen (920 °C for 3 h in argon) after fatigue tests at 95 MPa, $R = -1$. (a) Dissolution of the ferrite–cementite interface resulting in the formation of microvoids. 6.26×10^5 reversals; × 11 300. (b) Fracture of inclusion and formation of intrusion-type defects at hydrogen blisters. 1.05×10^6 reversals; × 11 300. (c) Formation of subgrains and microcracks at subgrain boundaries after 1.05×10^6 reversals; × 8200.

narrow region of varying width which was enriched in sulphur compared to the bulk of the matrix. In the absence of applied stress, corrosion occurred in this sulphur-enriched band resulting in the formation of micropits. Localized dissolution also occurred at the inclusion–matrix interfaces and, in the pearlitic regions, at the ferrite–cementite interfaces.

Under the influence of the cyclic stress, dissolution occurred more rapidly at the inclusion–matrix interfaces than under stress-free conditions. Cyclic stress also caused dissolution of the inclusions irrespective of the shape of the inclusions or of their manganese and iron content. With increasing number of reversals, or increasing stress, nucleation (Fig. 6) and coalescence of the microfissures occurred in the sulphur-enriched regions surrounding the inclusions. Fracture and undermining of some of the inclusions also occurred with increasing duration of stress, creating microvoids. In addition, microfissures appeared to nucleate from the tip of the inclusions. Linking of the microfissures and microvoids resulted in the formation of incipient cracks.

Previously [6], it was observed that on the application of cyclic stress, the pH at the mouth of the crevices and micropits on the surface of the fatigue-tested specimens became lower than that on the surface of the unstressed specimens. The reduction of the pH would stimulate the dissolution of the inclusions to produce more HS^-_{aq} ions which could accelerate the dissolution of the steel surface in the crevices or pits. This dissolution process produces fissures and crevices within the pits.

Sulphide inclusions also have sufficient solubility to produce a significant local concentration of H_2S and HS^-_{aq} ions [8]. In addition, chloride ions are able to diffuse toward regions of high stress, e.g. around inclusions, creating zones of high chloride-ion concentration [9]. Hence the activity of sulphide and chloride ions is higher near the inclusions than in the bulk solution. Additionally, the presence of H_2S in an aqueous solution greatly increases the amount of hydrogen absorbed by steel [4]. Thus the dissolution of sulphide enhances the local transport of hydrogen into the metal as a result of the presence of H_2S at the solution–inclusion interface.

Therefore, it appears that localized corrosion occurring at or near the inclusions nucleates pits which contain an acidic environment within them. As a consequence, dissolutions of the inclusions and metal occur with H_2S evolution. The presence of hydrogen blisters in the vicinity of the inclusions (Fig. 4a) suggests that hydrogen discharge takes place on the steel

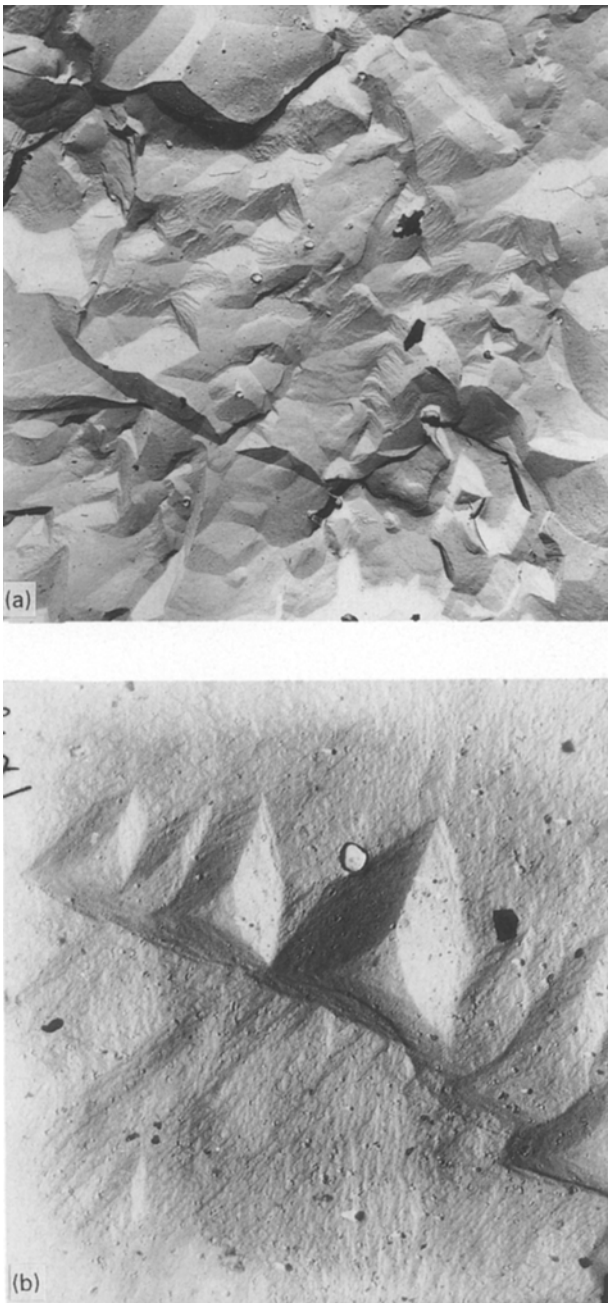

Figure 2 Transmission electron micrograph of an as-received specimen after fatigue tests at 95 MPa, $R = -1$. 1.05×10^6 reversals. (a) Deformed region with microcracks; $\times 2200$. (b) Etch pits in the deformed region (a); $\times 8200$.

surface as well as within the micro- and macropits and, under the influence of H_2S and HS^-_{aq} ions, the entry of hydrogen from the steel surface into the metal matrix is promoted. It also indicates the existence of microcracks and voids beneath the surface.

The localized activity within the micropits occurs at internal sulphide inclusions, pearlitic areas and at grain boundaries. Hydrogen absorption also occurs at dislocations, carbide–matrix interfaces and grain boundaries causing microvoids which enhances crack nucleation probabilities.

It is possible that if slip steps form in the metal within the crevices or pits, then as the pit opens, hydrogen atoms will be adsorbed on to the slip steps formed during the previous cycle. During the next cycle, the adsorbed hydrogen is swept in by the motion of mobile dislocations associated with the intrusion of the slip steps. This process is repeated during subsequent cycle. Because dislocations cannot travel from grain to grain, it is considered that the hydrogen-carrying dislocations must dump their load at or near the grain boundaries where the hydrogen atoms are then picked up by mobile dislocations originating near the grain boundary in the adjacent grain.

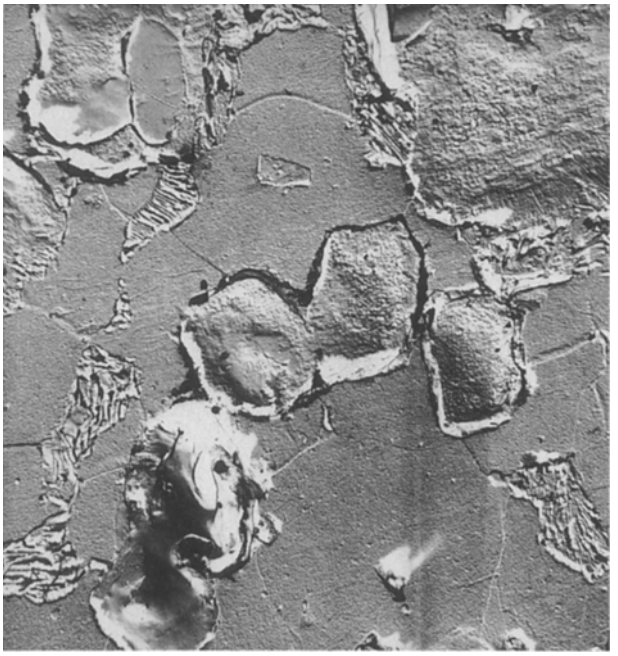

Figure 3 Transmission electron micrograph of fractured surface showing dissolution along grain boundaries and pearlitic regions. As-received specimen; 7.8×10^5 reversals at 179 MPa, $R = -1$; $\times 2192$.

It has, however, been suggested by Brown [10] that at rapid cycling rates and with full reversal of stress, hydrogen cracking is unlikely to occur, because hydrogen which may have tended to migrate to the effective sites during the tensile half-cycle is redistributed during compressive loading. It is considered that Brown's suggestion may be valid for extremely high frequencies. However, at the frequencies at which the specimens were fatigue tested in this investigation, the time for pick-up and dumping of hydrogen atoms at the grain boundaries is considered to be shorter than the fatigue cycle time. In addition, complete redistribution during compressive loading may be possible during full reversal of stress if a pit behaves like a crack. On closure of a crack, complete re-contact of opposing faces consisting of near perfect surfaces, may occur. However, the more open nature of the pits, and the imperfect surfaces of the opposing faces tend physically to obstruct interfacial re-contact between opposing walls and prevent complete closure of the pits during unloading and compressive reversal.

The difference between a crack and a pit is that whereas access of the environment to the crack tip is limited, in the case of pits, access of the environment is relatively easier and anodic dissolution and migration of hydrogen may be possible even during the complete reversal of stress because complete closure of the pit does not occur. The presence of hydrogen blisters

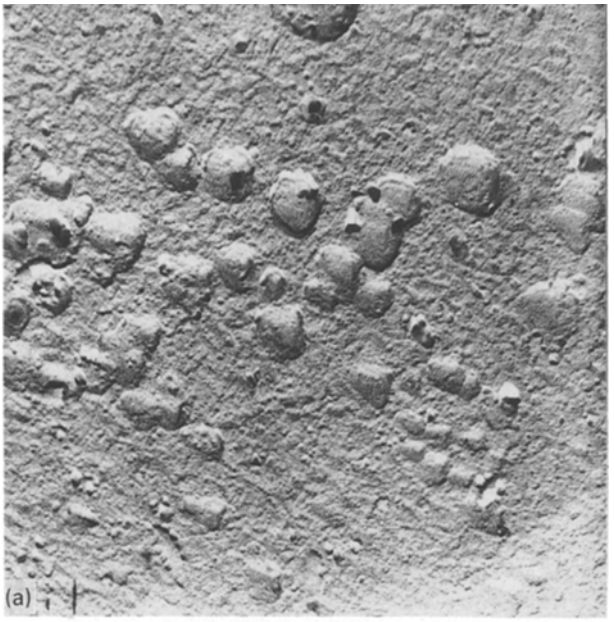

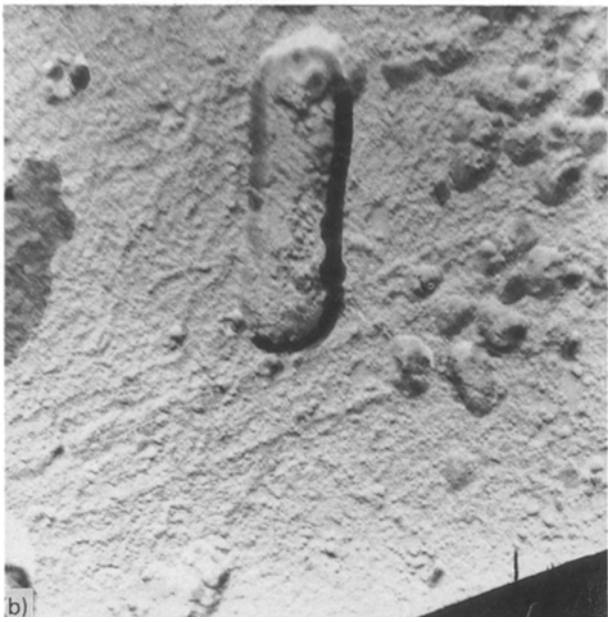

Figure 4 Transmission electron micrograph of an as-received specimen after 2000 reversals at 193 MPa, $R = -1$. (a) Formation of hydrogen blisters and submicroscopic cracks near inclusions; $\times 20\,500$. (b) Intersection of slip bands and hydrogen blisters; $\times 20\,500$.

(Figs 1b and 4) and microvoids with associated plastically deformed regions, indicates that effective redistribution of hydrogen during compressive loading is unlikely.

The development of micro- and macropits exposes a new volume of susceptible material resulting in the formation of microcavities. These microcavities extend towards the centre of the specimens due to dissolution along grain boundaries and pearlitic regions (Fig. 3). It is also possible that microvoid formation occurs at the grain and sub-grain boundaries and in the pearlitic regions due to the dynamic interaction of hydrogen with dislocation motion. Linking up of these microvoids takes place due to a stress-enhanced dissolution process.

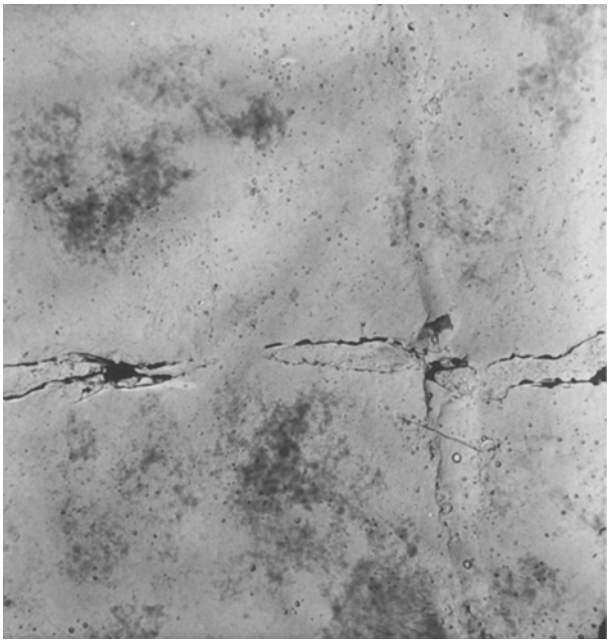

Figure 5 Transmission electron micrograph of an as-received specimen after 3.31×10^5 reversals at 247 MPa, $R = -1$, showing the formation of microcracks associated with the intersection of slip bands and inclusion; $\times 2200$.

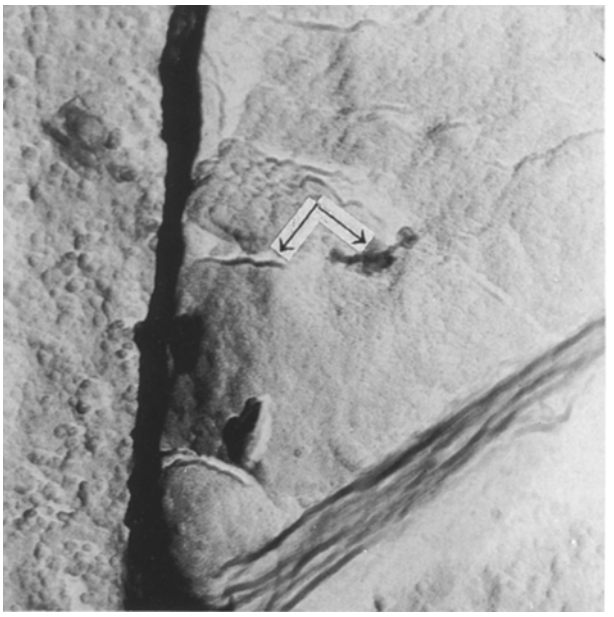

Figure 6 Transmission electron micrograph of an as-received specimen after 2000 reversals at 278 MPa, $R = -1$, showing dissolution at the inclusion–matrix interface and microfissure formation (arrowed) in the sulphur-enriched band surrounding the inclusion; $\times 40\,000$.

The lamellar structure in the pearlitic regions degenerates into ribbons of cementite, perforated lamellae, or even to isolated fragments (Fig. 1a) with the application of cyclic stress. Localized dissolution at the ferrite–cementite and pearlite colony–matrix interfaces appears to be enhanced with the formation of microvoids. Voids also form between the fractured ends of cementite lamellae under the influence of stress. Linking up of these voids appears to be the precursor of incipient crack formation in and around the pearlitic regions.

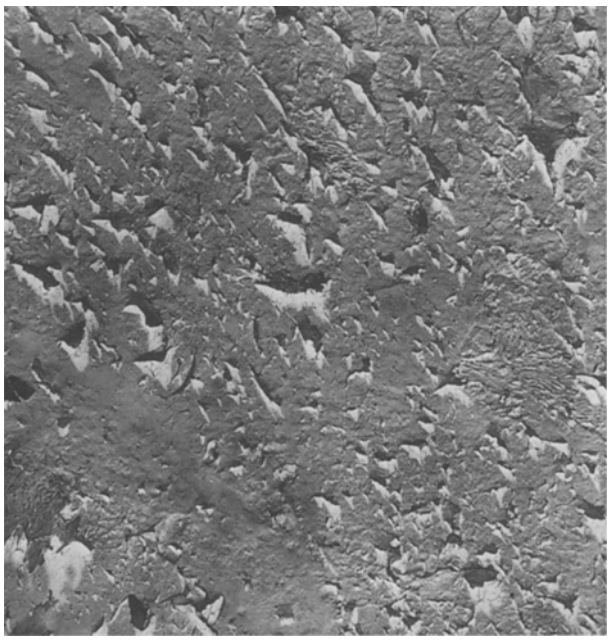

Figure 7 Transmission electron micrograph of an as-received specimen after 2×10^5 reversals at 309 MPa, $R = -1$, showing the formation of microvoids near the slip band; $\times 2200$.

Slip bands are found to occur in the matrix with increasing number of reversals. These bands also intersect inclusions (Fig. 5) and hydrogen blisters (Fig. 4b) causing voids from which cracks initiate. Additionally, microvoids were found in slip bands and in the matrix. It was observed that the individual microvoids do not grow, but that propagation occurs by linking. The linking of these microvoids results in the formation of microcracks in the slip bands and sub-grain boundaries.

Slip bands also form between the pearlitic regions on the specimen surface. Microcracks tend to develop at the edges of these bands possibly because of the localized dissolution which is easier from sites on the slip steps than from the unstepped crystal surface. These slip bands provide a path for linking the incipient cracks developed in the pearlitic areas. At higher stresses, slip bands appeared to intersect pearlitic regions resulting in the formation of incipient cracks.

Crack initiation also occurs with the formation of what may be termed pores or voids in areas where the microstructure is abnormally distorted [11]. Cottrell and Strutt [12], however, suggested that the pores were, in fact, etch pits developed at centres of strains such as dislocation tangles, and such tangles were characteristics of cyclic straining. In this investigation it was observed that under smaller stress amplitudes, slip concentration could give rise to distortion zones (Fig. 2a) consisting of etch pits (Fig. 2b) as well as microcracks. However, in the higher stress range, nucleation of microcracks or voids, as suggested by Wood [11], occurs in the disoriented regions near inclusions (Fig. 6) and slip bands (Fig. 7).

The nucleation of microcracks at grain boundaries may result from plastic strain and plastic folding at grain boundaries due to the differences in orientation between the adjoining grains. Because each grain has a different orientation, the distribution of strain between the grains is hindered at the grain boundaries. The constraining effects of grain boundaries and the inhomogeneity of strain distribution possibly accounts for the grain-boundary deformation. It is possible that the strain disparity in adjacent grains produces a squeezing action on the material near the deformed boundary, causing extrusion-like defects.

5. Conclusions

The study of the role of non-metallic inclusions in ferritic steel under condition of corrosion fatigue leads to the following conclusions.

1. The concentration of inclusions in steel differs from place to place. Nucleation and coalescence of micropits at inclusions and inclusion–matrix interfaces occur in both the high and low inclusion density regions.

2. Inclusions are surrounded by a narrow region of varying width which is enriched in sulphur compared to the bulk of the matrix. Corrosion occurs in these sulphur-enriched bands.

3. Cyclic stress enhances the nucleation and coalescence of micropits to form macropits at inclusions, inclusion–matrix interfaces and in the sulphur-enriched regions surrounding the inclusions.

4. Dissolution of the inclusions enhances local transport of hydrogen into the metal.

Under cyclic stress conditions, access of the environment is relatively easier in the pit than in the crack, and anodic dissolution and migration of hydrogen within the pit is possible even during complete reversal of stress, because complete closure of the pit does not occur. Hydrogen, therefore, plays a significant role in the nucleation of microcracks.

5. In the pearlitic areas, nucleation of micropits occurs at the cementite–ferrite and the pearlite colony–matrix interfaces. Linking up of these micropits nucleates incipient cracks in and around the pearlitic regions.

6. Slip bands form on the matrix, at the grain boundaries and between the pearlitic regions. Microvoids and microcracks tend to occur in and around the slip bands. Thus the formation of slip bands provides a path for linking of the incipient cracks formed in the pearlitic areas and assists the nucleation of microcracks. Generation of microcracks near the grain boundaries is also promoted by the presence of slip bands containing microvoids. Crack nucleation also occurs due to the intersection of slip bands and inclusions or pearlitic regions.

7. Microvoids nucleate on the matrix and linking up of these microvoids results in the formation of sub-boundaries and microcracks in the matrix.

8. Nucleation of microcracks was also found to occur at the grain boundaries.

Acknowledgements

The authors thank Dr M. Clarke, and Dr C. J. L. Booker, formerly of Sir John Cass School of Science and Technology, Department of Metallurgy and

Materials, City of London Polytechnic, London, for the provision of the laboratory facilities prior to the sad and ultimate closure of the Department in 1988. Their debt to the late Prof. L. L. Shreir is also acknowledged.

References

1. R. N. PARKINS, *Met. Technol.* **9** (1982) 122.
2. B. D. CRAIG, *Corrosion* **34** (1978) 282.
3. A. S. TETELMAN, in "Conference on the Fundamental Aspects of Stress Corrosion Cracking", Ohio State University, edited by R. W. Staehle, A. J. Forty and D. VanRooyen (NACE, Houston, Texas, 1967) p. 446.
4. A. KAWASHIMA, K. HASHIMOTO and S. SHIMODAIRA, *Corrosion* **32** (1976) 321.
5. G. P. RAY and R. A. JARMAN, *Br. Corros. J.* **15** (1980) 226.
6. G. P. RAY, R. A. JARMAN and J. G. N. THOMAS, *Corros. Sci.* **25** (1985) 171.
7. G. P. RAY, *Trans. Inst. Met. Finish.* **56** (1978) 168.
8. G. WRANGLEN, *Corros. Sci.* **14** (1974) 331.
9. C. PATEL, *Corrosion* **36** (1980) 665.
10. B. F. BROWN, in "Proceedings of the Conference on Corrosion Fatigue: Chemistry, Mechanics and Microstructure", University of Connecticut, edited by O. Devereux, A. J. McEvily and R. W. Staehle (NACE, Houston, Texas, 1971) p. 25.
11. W. A. WOOD, "Fracture", 1st Tewskbury Symposium, University of Melbourne, edited by C. Osborn (University of Melbourne, Melbourne, 1963) p. 62.
12. A. H. COTTRELL and P. R. STRUTT, *ibid.*, p. 74.

Received 1 May 1992
and accepted 24 February 1993